ELSEVIER

PII: S0032-3861(97)10355-X

Polymer Vol. 39 No. 16, pp. 3651–3656, 1998

0032-3861/98/$19.00+0.00

Excitation intensity-dependent fluorescence behaviour of some luminescent polymers

W. Holzer[a], A. Penzkofer[a,*], S.-H. Gong[a], D. D. C. Bradley[b], X. Long[b], W. J. Blau[c] and A. P. Davey[c]

[a]*Institut II-Experimentelle und Angewandte Physik, Universität Regensburg, D-93040 Regensburg, Germany*

[b]*Electronic and Photonic Molecular Materials Group, Department of Physics and Centre for Molecular Materials, The University of Sheffield, Hicks Building, Hounsfield Road, Sheffield S3 7RH, UK*

[c]*Department of Pure and Applied Physics, University of Dublin, Trinity College, Dublin 2, Ireland*

(Received 28 July 1997; revised 28 October 1997)

The fluorescence lifetime, fluorescence signal output and fluorescence spectral distribution of three highly diluted luminescent polymers (one para-phenylenevinylene and two para-phenylene-ethynylene polymers) in tetrahydrofuran are studied as a function of picosecond laser pulse excitation intensity. The results are compared with coumarin 2 in methanol and a distyrylbenzene molecule in tetrahydrofuran. The fluorescence lifetime and the spectral distribution are practically independent of excitation intensity, indicating the absence of excitation-dependent cooperative effects and the absence of emission from preferred exciton states. The fluorescence signal saturation of the polymer solutions at high excitation intensities indicates the photoexcitation of polymer segments (excitons or polarons) extending on average over two para-phenylene-ethynylene or four para-phenylenevinylene monomeric units.

(Keywords: conjugated polymers; fluorescence spectroscopy; saturation spectroscopy)

INTRODUCTION

Conjugated polymers have potential applications in electroluminescent optoelectronic devices[1,2]. Lasing in conjugated polymer solutions has been demonstrated[3–7], microcavity lasers have been realised[8,9], and stimulated emission in polymer films has been observed[9–12]. In the case of picosecond or nanosecond laser pumping of polymer solution lasers, high pump pulse energy densities are applied so that more than one photon per polymer is absorbed per excitation process. Multi-excited polymers are involved in short-pulse pumped polymer lasers[6,7].

The spectroscopic behaviour of three laser active polymers as a function of picosecond excitation pulse energy density is studied here. The excitation pulse energy density is varied from about a factor of a thousand below the monomeric saturation energy density to about a factor of ten above the monomeric saturation energy density. Polymer solutions of low concentration in a tilted cell were used to avoid amplified spontaneous emission[13,14]. The fluorescence lifetime and the fluorescence spectral distribution are found to be practically independent of the excitation energy density. The fluorescence signal saturation indicates the removal of two para-(phenylene-ethynylene) or four para-phenylenevinylene monomeric units out of the absorbing ground state per absorbed photon. The results give information on the exciton nature in the conjugated polymer chains[1,15]. For comparison, the spectroscopic behaviour of the organic dye coumarin 2 dissolved in methanol and of t,t′-(didecyloxy)-II-distyrylbenzene dissolved in tetrahydrofuran is studied under the same experimental conditions as applied to the polymer solutions. The distyrylbenzene molecule is a model compound for the para-phenylenevinylene polymer.

EXPERIMENTAL

The polymers poly(m-phenylenevinylene-co-2,5-dioctoxy-p-phenylenevinylene) (abbreviated PmPV-co-DOctOPV)[6], poly(2,5-dioctadecyloxy-paraphenylene-ethynylene-co-2,5-thienyl) (OPT)[7,16], and poly(2,5-dioctadecyloxy-paraphenylene-ethynylene-co-2,5-pyridinyl) (OPP)[7,16] were investigated. The degrees of polymerisation, n_{pol}, and the polydispersivities, n_{dis},[17] are listed in *Table 1*. The polymers were dissolved in tetrahydrofuran (THF). For comparison, the organic dye coumarin 2 in methanol and the model compound t,t′-(didecyloxy)-II-distyrylbenzene (DDO-DSB) were investigated. The structural formulae are displayed in *Figure 1*. The monomeric absorption cross-section spectra of the compounds are displayed in *Figure 2*.

The experimental arrangement is shown in *Figure 3*. The excitation pulses were generated in an active and passive mode-locked and frequency-doubled ruby laser system with a single pulse selector and an amplifier (wavelength 347.15 nm, duration Δt_P (≈ 35 ps, energy up to 1.5 mJ)[18]. The fundamental laser pulse was blocked off with a short-pass filter, EF. The laser beam diameter, Δd_P, was reduced with lens L1 to $\Delta d_P = 1.3$ mm (FWHM). The pump pulse energy was varied with neutral density filters, F1. Corresponding neutral density filters, F2–F4, were used in

* To whom correspondence should be addressed

Table 1 Spectroscopic parameters (room temperature)

Solute Solvent	PmPV-co-DOctOPV THF	OPT THF	OPP THF	DDO-DSB THF	Coumarin 2 Methanol	Comments
n_{pol}	33[a]	81[b]	27[b]			
n_{dis}	2.5[a]	1.7[b]	5.6[b]			
C_m (mol/dm^3)	5.1×10^{-5}	1.89×10^{-4}	1.34×10^{-4}	2.59×10^{-5}	1.52×10^{-4}	
$N_{m,0}$ (cm^{-3})	3.06×10^{16}	1.14×10^{17}	8.06×10^{16}	1.16×10^{16}	9.17×10^{16}	
$\sigma_{P,m}$ (cm^2)	7.5×10^{-17}	4.54×10^{-17}	5.8×10^{-17}	7.91×10^{-17}	5.9×10^{-17}	Figure 2
$w^{sat}_{P,m}$(J/cm^2)	7.63×10^{-3}	1.26×10^{-2}	9.87×10^{-3}	7.24×10^{-3}	9.7×10^{-3}	equation (1)
$w^{sat}_{P,pol}$ (J/cm^2)	2.3×10^{-4}	1.56×10^{-4}	3.66×10^{-4}			equation (2)
τ_F (ns)	1.7 ± 0.2	0.75 ± 0.2	1.0 ± 0.2	1.85 ± 0.2	3.6 ± 0.3	
ϕ_F	0.64[a]	0.39[b]	0.46[b]	0.645 ± 0.02	0.74 ± 0.03[c]	
$\sigma_{ex,P}/\sigma_P$	0.83[d]	0.88[e]	0.69[e]	0.32 ± 0.03	1.1[f]	
τ_{FC} (ps)	0.5	0.5	0.5	0.5	0.5	assumed[34]
$\tau_{ex,P}$ (fs)	60	60	60	60	60	assumed[35]
τ_v (ps)	4	4	4	4	4	assumed[36]
τ_{rad} (ns)	2.7 ± 0.5	1.9 ± 0.6	2.2 ± 0.5	2.9 ± 0.4	4.9 ± 0.5	equation (3)
$\tau^{SB}_{rad,m}$ (ns)	3.6	3.5	3.2	2.8	5.3	equation (4)
λ_a (nm)	352	353	351	350	275	Figure 2
λ_b (nm)	480	500	500	480	450	Figure 2

[a]Ref. [6]
[b]Ref. [7]
[c]Value misprinted in Refs [6,37]
[d]Ref. [38]
[e]Ref. [39]
[f]Ref. [37]

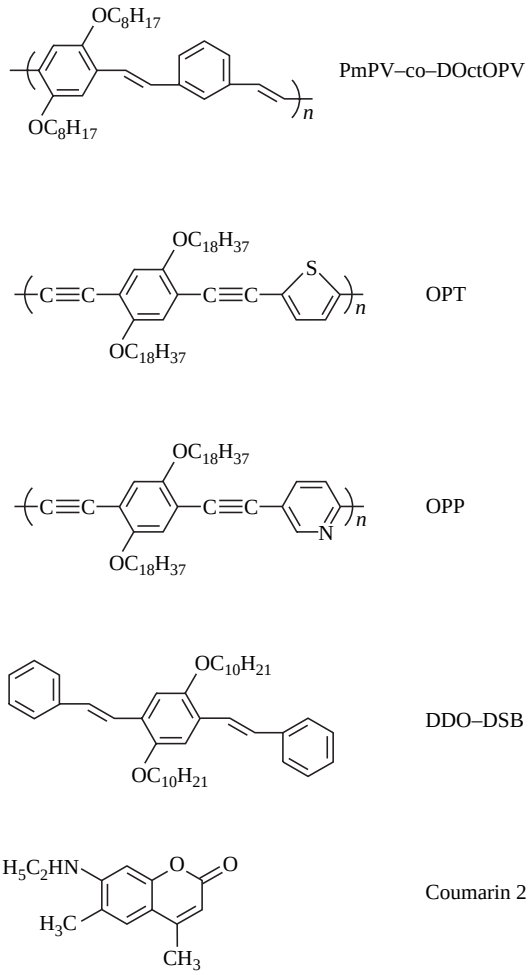

Figure 1 Structural formulae of investigated polymers, model molecule and organic laser dye. PmPV-co-DOctOPV, poly(m-phenylenevinylene-co-2,5-dioctoxy-p-phenylenevinylene; OPT, poly(2,5-dioctadecyloxy-paraphenylene-ethynylene-co-2,5-thienyl; OPP, poly(2,5-dioctadecyloxy-paraphenylene-ethynylene-co-2,5-pyridinyl; DDO-DSB, t,t-(didecyloxy)-II-distyrylbenzene. Coumarin 2, 7-amino-4-methylcoumarin

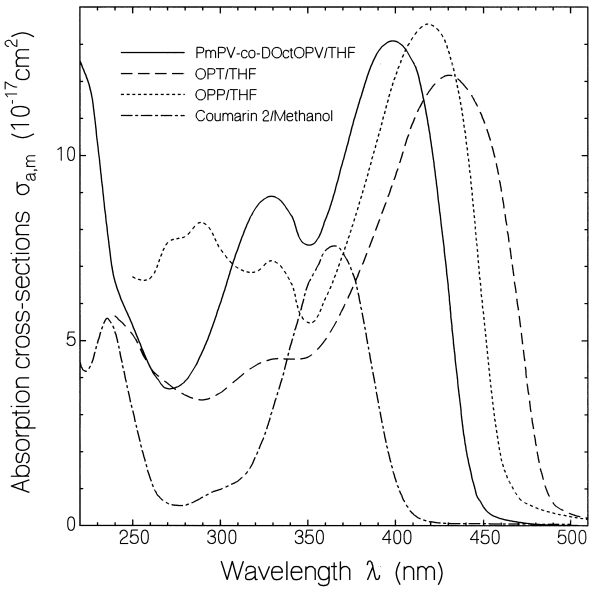

Figure 2 Monomeric absorption cross-section spectra, $\sigma_{a,m}(\lambda)$, of investigated samples. $\sigma_{a,m}(\lambda) = \alpha(\lambda)/N_{m,0}$ where $\alpha(\lambda)$ is the absorption coefficient and $N_{m,0}$ is the monomeric number density

front of the detectors. The photodetector PD measured the input pump pulse energy. The spectral distribution of the fluorescence emission was measured with a spectrometer-diodearray detection system. Part of the sideward emitted fluorescence light was collected with lens L2 and was imaged to the spectrometer entrance with lens L3. The temporal fluorescence emission was monitored with a microchannel-plate photomultiplier (Hamamatsu type R1564U) and a fast digital oscilloscope (LeCroy type 9362). The fluorescence lifetime was determined by deconvoluting the fluorescence signal decay from the pump laser signal response. The total fluorescence emission was proportional to the time integrated oscilloscope trace.

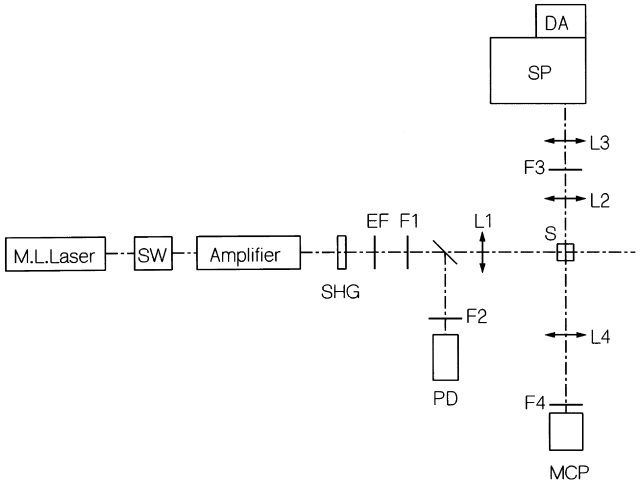

Figure 3 Experimental set-up. M.L.Laser, active and passive mode-locked ruby laser; SW, electro-optic single pulse selector; Amplifier, double-pass ruby laser amplifier; SHG, ADP crystal for second harmonic generation; EF, short-pass filter (blocks fundamental laser frequency); F1–F4, neutral density filters; L1–L4, lenses; S, sample cell of 1.5 mm × 1.5 mm inner cross-section; PD, photodetector; MCP, multichannel-plate photomultiplier; SP, spectrometer; DA, diode-array detection system

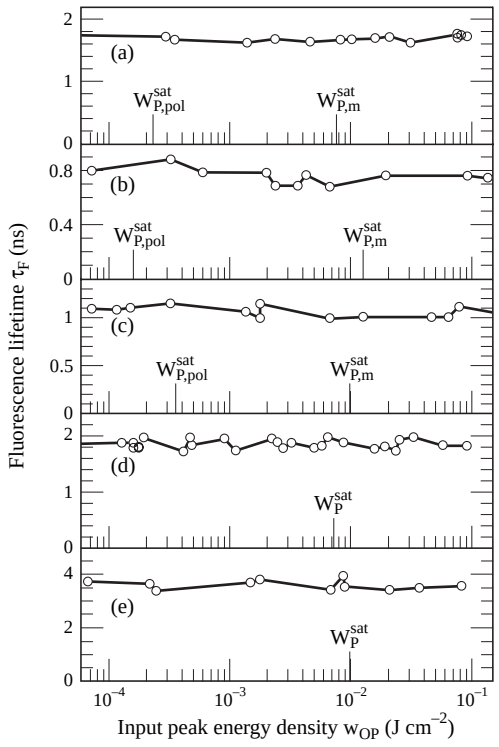

Figure 4 Experimental fluorescence lifetime, τ_F, *versus* input pump pulse energy density, w_{0P}, for PmPV-co-DOctOPV in THF (a); OPT in THF (b); OPP in THF (c); DDO-DSB in THF (d); and coumarin 2 in methanol (e). Concentrations are listed in *Table 1*

RESULTS

The fluorescence lifetimes, spectral fluorescence distributions, and time-integrated fluorescence signal outputs were determined as a function of the pump pulse energy density. The pump pulse energy densities were varied with neutral density filters over a wide range from approximately one thousandth below the monomeric saturation energy density, $w_{P,m}^{sat}$ up to approximately a factor of ten above the monomeric saturation energy density.

The monomeric saturation energy density, $w_{P,m}^{sat}$ is given by[19]

$$w_{P,m}^{sat} = \frac{h\nu_P}{\sigma_{P,m}} \quad (1)$$

where h is the Planck constant, ν_P is the pump laser frequency, and $\sigma_{P,m} = \alpha_P/N_{m,0}$ is the monomeric absorption cross-section at the pump laser frequency. $\alpha_P = -\ln(T_0)/l$ is the absorption coefficient and $N_{m,0} = N_{pol,0}n_{pol}$ is the number density of monomeric units. $N_{pol,0}$ is the number density of polymer chains and n_{pol} is the degree of polymerisation. T_0 is the small-signal transmission, and l is the sample length. equation (1) is valid for our experimental situation of slow saturable absorption, where the pump pulse duration, Δt_P, is short compared with the fluorescence lifetime, τ_F [20].

At $w_P = w_P^{sat}$ half of the absorbing entities are excited in the case of thin absorption conditions ($|\ln(T_0)| \ll 1$) [19]. For thick saturable absorbers ($|\ln(T_0)| \gtrsim 1$) the pump pulse energy density necessary for exciting half of the absorbing entities is approximately given by

$$\begin{aligned} w_P &\approx w_P^{sat}[1 + 0.5N_{m,0}lh\nu_P/w_{P,m}^{sat}] \\ &= w_P^{sat}[1 - 0.5\ln(T_0)h\nu_P/(\sigma_{P,m}w_{P,m}^{sat})] \\ &= w_P^{sat}[1 - 0.5\ln(T_0)]. \end{aligned}$$

In this approximation excited state absorption was neglected.

For the polymer solutions we defined a polymer saturation energy density, $w_{P,pol}^{sat}$ by

$$w_{P,pol}^{sat} = \frac{w_{P,m}^{sat}}{n_{pol}} = \frac{h\nu_P}{\sigma_{P,m}n_{pol}}. \quad (2)$$

At $w_P = w_{P,pol}^{sat}$ a chromophore is excited on average in every second polymer chain.

The fluorescence lifetimes *versus* input pump pulse energy density are displayed in *Figure 4* for the three polymer samples investigated, the dye sample, and the model compound. The saturation energy densities, $w_{P,m}^{sat}$ and $w_{P,pol}^{sat}$, are indicated. Within our experimental accuracy the fluorescence lifetimes were found to be independent of the excitation energy density for all investigated samples. Multiple chromophore excitation in the polymer chains did not influence the fluorescence lifetime.

The radiative lifetimes, τ_{rad}, determined from fluorescence lifetime, τ_F, and fluorescence quantum yield, ϕ_F, measurements are listed in *Table 1*. The relation:

$$\tau_{rad} = \frac{\tau_F}{\phi_F} \quad (3)$$

was used. Additionally the radiative lifetimes, $\tau_{rad,m}^{SB}$, determined from the monomeric absorption spectra (*Figure 2*, $\sigma_a(\lambda) = \sigma_{a,m}(\lambda)$, $n_{chr} = 1$) using the Strickler–Berg formula[21,22]

$$\frac{1}{\tau_{rad,m}^{SB}} = \frac{8\pi c_0 n_F^3}{n_A} \frac{\int_{em} E_F(\lambda)d(\lambda)}{\int_{em} E_F(\lambda)\lambda^3 d\lambda} \int_{\lambda_a}^{\lambda_b} \frac{\sigma_{a,m}(\lambda)}{\lambda} d\lambda \quad (4)$$

are listed in *Table 1*. c_0 is the speed of light in vacuum, n_F and n_A are the average refractive indices of the solutions in the fluorescence and absorption region, respectively. The integrals extend over the emission wavelength region (em) and over the S_0–S_1 absorption band (wavelength borders λ_a and λ_b). τ_{rad} is somewhat shorter than $\tau_{rad,m}^{SB}$ for the polymer

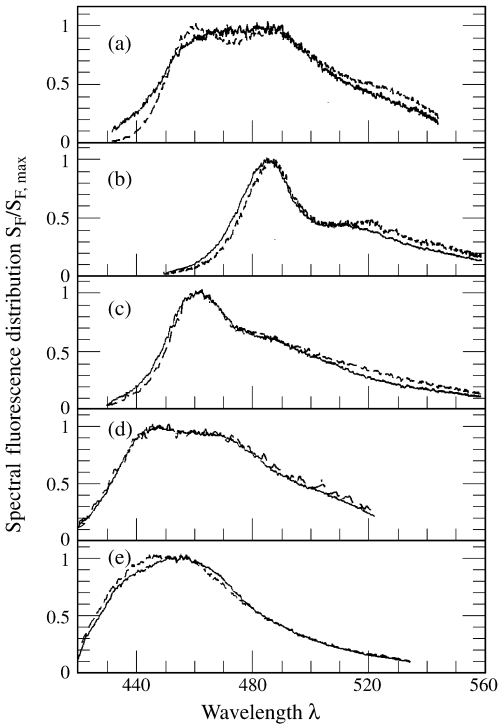

Figure 5 Normalised spectral fluorescence distributions, $S_F(\lambda)/S_{F,max}$. Concentrations are listed in *Table 1*. The spectra are uncorrected for the spectral sensitivity of the spectrometer-detector system. (a) PmPV-co-DOctOPV in THF. Solid curve, pump pulse peak energy density, $w_{0P} = 7.6 \times 10^{-2}$ J/cm^2 = $10 w_{P,m}^{sat}$. Dashed curve, $w_{0P} = 3.5 \times 10^{-5}$ J/cm^2 = $4.6 \times 10^{-3}\, w_{P,m}^{sat}$. (b) OPT in THF. Solid curve, $w_{0P} = 7.6 \times 10^{-2}$ J/cm^2 = $6\, w_{P,m}^{sat}$. Dashed curve, $w_{0P} = 4.1 \times 10^{-5}$ J/cm^2 = $3.3 \times 10^{-3}\, w_{P,m}^{sat}$. (c) OPP in THF. Solid curve, $w_{0P} = 0.167$ J/cm^2 = $17\, w_{P,m}^{sat}$. Dashed curve, $w_{0P} = 2.3 \times 10^{-5}$ J/cm^2 = $2.4 \times 10^{-3}\, w_{P,m}^{sat}$. (d) DDO-DSB in THF. Solid curve, $w_{0P} = 8.9 \times 10^{-2}$ J/cm^2 = $12.3\, w_{P,m}^{sat}$. Dashed curve, $w_{0P} = 9.7 \times 10^{-4}$ J/cm^2 = $8.1 \times 10^{-2}\, w_P^{sat}$. (e) Coumarin 2 in methanol. Solid curve, $w_{0P} = 0.09$ J/cm^2 = $9.3\, w_P^{sat}$. Dashed curve, $w_{0P} = 5 \times 10^{-5}$ J/cm^2 = $5.2 \times 10^{-3}\, w_P^{sat}$

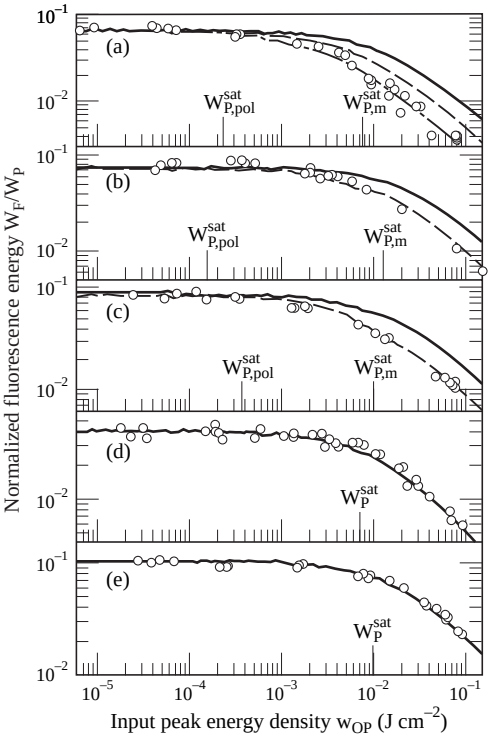

Figure 6 Normalised fluorescence energy, W_F/W_P, *versus* input pump pulse peak energy density, w_{0P}. Circles, experimental results adjusted at low pump pulse energy density to theoretical curves. Solid curves, calculated for monomeric chromophore size. Dashed curves, calculated for dimeric chromophore size. Dash-dotted curve, calculated for tetramer chromophore size. Applied parameters are listed in *Table 1*. (a) PmPV-co-DOctOPV in THF; (b) OPT in THF; (c) OPP in THF; (d) DDO-DBS in THF; (e) coumarin 2 in methanol

solutions indicating an extension of the emitting chromophore beyond the monomer size up to two monomer units.

In *Figure 5* fluorescence spectra at high excitation energy density, $w_P \approx 10 w_{P,m}^{sat}$ (solid curves), and at low excitation energy densities, $w_P < 0.1 w_{P,m}^{sat}$ (dashed curves), were compared. There were only slight spectral changes observed for all compounds. The largest spectral change were observed for PmPV-co-DOctOPV, where the double-peak structure observed at low excitation energies was somewhat smeared out at high excitation energies.

In *Figure 6* the normalised fluorescence energy, W_F/W_P, *versus* input pump pulse peak energy density, w_{0P}, is plotted for the polymer solutions, the dye solution, and the model molecule. W_F is the total emitted fluorescence energy (integration over all emission directions), and W_P is the input pump pulse energy. At low input pump pulse energy densities the experimental data points (circles) are adjusted to calculated curves (see below). Up to $w_{0P} \approx 0.1 w_{P,m}^{sat}$ the normalised fluorescence energy, W_F/W_P is approximately constant. Then a saturation occurs which lowers W_F/W_P, since the fluorescence signal is proportional to the number of excited chromophores and the excited chromophore number density cannot rise further with pump pulse energy density when all chromophores are already excited.

NUMERICAL SIMULATIONS

The normalised fluorescence energy, W_F/W_P, is calculated numerically in order to obtain information on the absorbing and emitting entities by comparison with the experimental data.

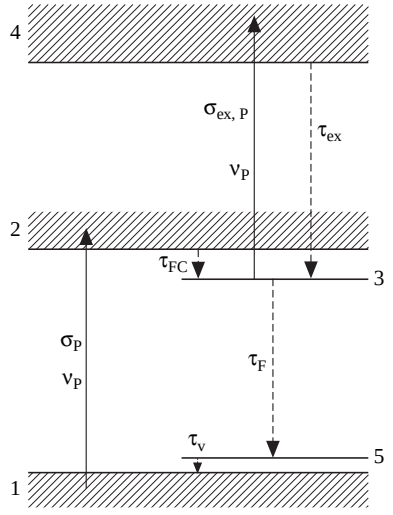

Figure 7 Energy band diagram used in fluorescence saturation calculations

The excitation and emission dynamics are described by a band model depicted in *Figure 7*. The pump pulse excites chromophores from band 1 (valence band, S_0-ground state) to band 2 (conduction band, S_1-band). From there the chromophores relax quickly to a chain relaxed state 3 (Franck–Condon relaxation time τ_{FC}). From states 2 and 3 excited-state absorption occurs to a higher lying band 4 (excited-state absorption cross-section, $\sigma_{ex,P}$). A fast excited-state relaxation (time constant τ_{ex}) occurs back to

level 3. (The excited-state absorption includes the removal of electrons from orbitals (bands) below the valence band (S_0-band) by excitation to the valence band (S_0-band) and fast relaxation of electrons from the valence band (S_0-band) to the generated hole states). From level 3 the chromophores relax with the fluorescence lifetime, τ_F, to level 5 and return to the ground-state (time constant $\tau_v \ll \tau_F$).

The relevant differential equation system for the absorption and emission dynamics reads[23,24]:

$$\frac{\partial N_1}{\partial t'} = \frac{3\sigma_P \cos^2(\theta)}{h\nu_P}(N_1 - N_2)I_P + \frac{N_5}{\tau_v} - \frac{N_1 - \bar{N}_1}{\tau_{or}} \quad (5)$$

$$\frac{\partial N_1}{\partial t'} = \frac{3\sigma_P \cos^2(\theta)}{h\nu_P}(N_1 - N_2)I_P - \frac{3\sigma_{ex,P}\cos^2(\theta)}{h\nu_P}\left(N_2 - \frac{N_2}{N_2 + N_3}N_4\right)I_P - \frac{N_2}{\tau_{FC}} - \frac{N_2 - \bar{N}_2}{\tau_{or}} \quad (6)$$

$$\frac{\partial N_3}{\partial t'} = \frac{N_2}{\tau_{FC}} - \frac{3\sigma_{ex,P}\cos^2(\theta)}{h\nu_P}\left(N_3 - \frac{N_3}{N_2 + N_3}N_4\right)I_P + \frac{N_4}{\tau_{ex}} - \frac{N_3}{\tau_F} - \frac{N_3 - \bar{N}_3}{\tau_{or}} \quad (7)$$

$$\frac{\partial N_4}{\partial t'} = \frac{3\sigma_{ex,P}\cos^2(\theta)}{h\nu_P}(N_3 - N_4)I_P - \frac{N_4}{\tau_{ex}} - \frac{N_4 - \overline{N}_4}{\tau_{or}} \quad (8)$$

$$\frac{\partial N_5}{\partial t'} = \frac{N_3}{\tau_F} - \frac{N_5}{\tau_v} - \frac{N_5 - \bar{N}_5}{\tau_{or}} \quad (9)$$

$$\frac{\partial I_P}{\partial z'} = -3\sigma_P\cos^2(\theta)(N_1 - N_2)I_P - 3\sigma_{ex,P}\cos^2(\theta)(N_3 - N_4)I_P \quad (10)$$

$$\bar{N}_i = \int_0^{\pi/2} N_i(\theta)\sin(\theta)d\theta, \; i = 1, 2, 3, 4, 5. \quad (11)$$

The absorption anisotropy is taken into account using $\sigma(\theta) = 3\sigma\cos^2(\theta)$, where θ is the angle between the polarisation of the excitation light and the orientation of the transition dipole moments of the chromophores[25]. τ_{or} is the reorientation time of the transition dipole moments. $\bar{N}_i$ is the orientation averaged level population number density of level i (i = 1, 2, 3, 4, 5). In the equation system the transformations $t' = t - nz/c_0$ and $z' = z$ are used, where t is the time, n is the refractive index, z is the propagation distance, and c_0 is the vacuum light velocity.

The initial conditions are

$$N_1(t' = -\infty, \theta, r, z') = \frac{N_{m,0}}{n_{chr}} \quad (12)$$

$$N_2(t' = -\infty, \theta, r, z') = N_3(t' = -\infty, \theta, r, z') = N_4(t' = -\infty, \theta, r, z') = N_5(t' = -\infty, \theta, r, z') = 0 \quad (13)$$

and

$$I_P(t', r, z' = 0) = I_{0P}\exp(-r^2/r_{0P}^2)\exp(-t'^2/t_{0P}^2), \quad (14)$$

where r is the radial coordinate, $t_{0P} = 2^{-1}[\ln(2)]^{-1/2}\Delta t_P$ is half the $1/e$-pulse width and $r_{0P} = 2^{-1}[\ln(2)]^{-1/2}\Delta d_P$ is the $1/e$-beam radius. Δt_P is the FWHM pulse duration, and Δd_P is the FWHM beam diameter. $N_{m,0}$ is the total number density of monomer units. n_{chr} is the number of monomers forming a chromophore (number of monomers removed from ground state in a single absorption process of one photon). The corresponding σ_P in the equation system is given by $\sigma_{P,chr} = n_{chr}\sigma_{P,m}$.

A numerical solution of the equation system [equations (5)–(11)] with the initial conditions [equations (12)–(14)] allows the determination of the population number density, $\bar{N}_3(t_e, r, z)$ of the emitting level 3 after passage of the pump pulse (time t_e). This population number density is needed for calculation of the total emitted fluorescence energy. The total fluorescence energy, W_F, normalised to the input pulse energy, W_P, is given by:

$$\frac{W_F}{W_P} = \frac{h\nu_F\phi_F \int_0^\infty \left[\int_0^l \bar{N}_3(t_e, r, z)dz\right] 2\pi r \, dr}{w_{0P}\int_0^\infty \exp(-r^2/r_{0P}^2)2\pi r \, dr} \quad (15)$$

where h is the Planck constant, ν_F is the mean frequency of the fluorescence light, ϕ_F is the fluorescence quantum yield, and l is the sample length. $w_{0P} = I_{0L}\int_{-\infty}^{\infty}\exp(-t^2/t_{0P}^2)dt$ is the peak input pulse energy density. Calculated W_F/W_P curves are shown in *Figure 6*. The parameters used in the calculations are listed in *Table 1*.

DISCUSSION

In *Figure 6* a comparison of the experimental fluorescence energy data with the calculated fluorescence energy curves allows the determination of the chromophore sizes. For PmPV-co-DOctPV in THF it is $n_{chr} = 4$. This means that one absorbed pump pulse photon removes four monomer units out of the absorbing ground state position. The lattice relaxation after absorption of one photon removes a polymer segment, consisting, on average, of four monomer units, out of its original energy position. For OPT in THF and OPP in THF it is $n_{chr} = 2$, i.e., one absorbed pump photon removes a segment extending on average over to two monomer units out of its original absorbing position. For the monomeric dye coumarin 2 in methanol and for the distyrylbenzene molecules it is $n_{chr} = 1$. One absorbed photon removes one molecule from the ground-state position.

The fluorescence spectra displayed in *Figure 5* are practically independent of the excitation energy densities. This means that the emission spectrum is independent of how many chromophores (lattice relaxed segments) are excited in a polymer chain. This behaviour provides no indication of relaxation to preferred low-lying emitting states in the polymer chains at low excitation intensities. Excitation migration in polymer chains hardly alters the emission spectrum.

The measured fluorescence lifetimes have been found to be independent of the excitation energy density for all samples investigated (*Figure 4*). This finding indicates that no cooperative emitting states are formed in the case of simultaneous multiple excitation of the polymer chains. For the polymer solutions the radiative lifetimes, τ_{rad}, determined from the fluorescence lifetime and fluorescence quantum yield measurements are somewhat shorter (a factor of 0.5–0.8) than the radiative lifetimes, $\tau_{rad,m}^{SB}$, determined

from the monomeric absorption spectra [$\sigma_a(\lambda) = \sigma_{a,m}(\lambda)$, $n_{chr} = 1$] using the Strickler–Berg formalism[21,22] (*Table 1*). The coherence length of the excitation (exciton or polaron exciton[15]) on average is limited to one to two monomeric units[26–29].

CONCLUSIONS

The fluorescence behaviour of three conjugated polymers, a model compound, and an organic dye has been measured as a function of excitation energy density. Diluted solutions were studied to avoid amplified spontaneous emission effects. The fluorescence lifetimes and the fluorescence spectral shapes were found to be practically independent of the excitation energy density. The saturation behaviour of the fluorescence signals indicates that photoexcitation forms lattice relaxed segments. For two polymers (OPT and OPP) the segments extend on average over two monomeric units, and for the third investigated polymer (PmPV-co-DOctOPV) an average segment extension over four monomeric units was found. The independence of the fluorescence lifetime on multiple excitation of polymer chains indicates the absence of cooperative emission like superradiance[30–32] or superfluorescence[31–33]. The independence of spectral fluorescence distribution on multiple polymer chain excitation indicates the absence of preferred emission from a low-lying exciton state in the polymer chains.

REFERENCES

1. Greenham, N. C. and Friend, R. H., in *Solid State Physics*, Vol. 49, ed. H. Ehrenreich and F. Spaepen. Academic Press, San Diego, 1995, p. 2.
2. Mark, J. E. (ed.), *Physical Properties of Polymers Handbook*. American Institute of Physics, New York, 1996.
3. Moses, D., *Appl. Phys. Lett.*, 1992, **60**, 3215.
4. Brouwer, H. J., Krasnikov, V. V., Hilberer, A., Wildman, J. and Hadziioannou, G., *Appl. Phys. Lett.*, 1995, **66**, 3404.
5. Hide, F., Schwartz, B. J., Díaz-García, M. A. and Heeger, A. J., *Chem. Phys. Lett.*, 1996, **256**, 424.
6. Holzer, W., Penzkofer, A., Gong, S.-H., Bleyer, A. and Bradley, D. D. C., *Adv. Mater.*, 1996, **8**, 974.
7. Holzer, W., Penzkofer, A., Gong, S.-H., Davey, A. P. and Blau, W. J., *Opt. Quant. Electron*., 1997, **29**, 713.
8. Tessler, N., Denton, G. J. and Friend, R. H., *Nature*, 1996, **382**, 695.
9. Díaz-García, M. A., Hide, F., Schwartz, B. J., McGehee, M. D., Anderson, M. R. and Heeger, A. J., *Appl. Phys. Lett.*, 1997, **70**, 3191.
10. Hide, F., Díaz-García, M. A., Schwartz, B. J., Anderson, M. R., Pei, Q. and Heeger, A. J., *Science*, 1996, **273**, 1833.
11. Brouwer, H. J., Krasnikov, V. V., Hilberer, A. and Hadziioannou, G., *Adv. Mater.*, 1996, **8**, 935.
12. Hide, F., Díaz-García, M. A. and Heeger, A. J., *Laser Focus World*, 1997, **33**, 151.
13. Svelto, O., *Principles of Lasers*, 3rd edn. Plenum Press, New York, 1993.
14. Penzkofer, A. and Blau, W., *Opt. Quant. Electron.*, 1983, **15**, 325.
15. Heeger, A. J., Kivelson, S., Schrieffer, J. R. and Su, W.-P., *Rev. Mod. Phys.*, 1988, **60**, 781.
16. Davey, A. P., Elliott, S., O'Connor, O. and Blau, W., *J. Chem. Soc. Chem. Commun.*, 1995, 1433.
17. Determann, H., *Gelchromatographie*. Springer, Berlin, 1967.
18. Weidner, P. and Penzkofer, A., *Opt. Quant. Electron.*, 1993, **35**, 1.
19. Hercher, M., *Appl. Opt.*, 1967, **6**, 947.
20. Bäumler, W. and Penzkofer, A., *Opt. Quant. Electron.*, 1991, **23**, 439.
21. Strickler, S. J. and Berg, R. A., *J. Chem. Phys.*, 1962, **37**, 814.
22. Birks, J. B. and Dyson, D. J., *Proc. Roy. Soc. London, Ser A*, 1963, **275**, 135.
23. Penzkofer, A. and Falkenstein, W., *Opt. Quant. Electron.*, 1978, **10**, 399.
24. Penzkofer, A., Beidoun, A. and Daiber, M., *J. Luminesc.*, 1992, **51**, 297.
25. Cehelnik, E. D., Mielenz, K. D. and Velapoldi, R. A., *J. Res. Nat. Bureau Standards A—Phys. and Chem.*, 1975, **79**, 1.
26. Herz, A. H., *Adv. in Colloid and Interface Science*, 1977, **8**, 237.
27. Möbius, D., *Adv. Mater.*, 1995, **7**, 437.
28. Knapp, E. W., *Chem. Phys.*, 1984, **85**, 73.
29. Fidder, H., Knoester, J. and Wiersma, D. A., *J. Chem. Phys.*, 1993, **98**, 6564.
30. Dicke, R. H., *Phys. Rev.*, 1954, **93**, 99.
31. Shen, Y. R., *The Principles of Nonlinear Optics*. Wiley, New York, 1984.
32. Schubert, M. and Wilhelmi, B., *Nonlinear Optics and Quantum Electronics*. Wiley Interscience, New York, 1986.
33. Bonifacio, R. and Lugiato, L., *Phys. Rev. A*, 1975, **11**, 1507.
34. Penzkofer, A., Falkenstein, W. and Kaiser, W., *Chem. Phys. Lett.*, 1976, **44**, 82.
35. Graf, F. and Penzkofer, A., *Opt. Quant. Electron.*, 1989, **17**, 53.
36. Seilmeier, A. and Kaiser, W., in *Ultrashort Laser Pulses and Applications*, ed. W. Kaiser. Vol. 60, *Topics in Applied Physics*. Springer, Berlin, 1988, p. 279.
37. Penzkofer, A., Holzer, W. and Gong, S.-H., *Opt. Quant. Electron.*, 1997, **29**, 611.
38. Holzer, W., Penzkofer, A., Gong, S.-H., Bradley, D. D. C., Long, X. and Bleyer A., *Chem. Phys.*, 1997, **224**, 315.
39. Holzer, W., Penzkofer, A., Gong, S.-H., Blau, W. J. and Davey, A. P., Effective stimulated emission and excited-state absorption cross-section spectra of para-(phenylene-ethynylene) polymers. *Opt. Quant. Electron*., 1998, **30**, in press.